Probing the Hard Segment Phase Connectivity and Percolation in Model Segmented Poly(urethane urea) Copolymers

ARTICLE *in* MACROMOLECULES · JUNE 2005

Impact Factor: 5.8 · DOI: 10.1021/ma048222v

5 AUTHORS, INCLUDING:

Ann Fornof
Ludwig-Maximilians-University of Munich
21 PUBLICATIONS **404** CITATIONS
SEE PROFILE

Iskender Yilgor
Koc University
135 PUBLICATIONS **3,036** CITATIONS
SEE PROFILE

Probing the Hard Segment Phase Connectivity and Percolation in Model Segmented Poly(urethane urea) Copolymers

Jignesh P. Sheth and Garth L. Wilkes*

Department of Chemical Engineering, Virginia Polytechnic Institute and State University, Blacksburg, Virginia 24061

Ann R. Fornof and Timothy E. Long

Department of Chemistry, Virginia Polytechnic Institute and State University, Blacksburg, Virginia 24061

Iskender Yilgor

Department of Chemistry, Koc University, Istanbul 34450, Turkey

Received August 31, 2004; Revised Manuscript Received January 31, 2005

ABSTRACT: Soluble model segmented poly(urethane urea)s (PUU) with or without hard segment (HS) branching were utilized to explore the importance of hydrogen bonding and chain architecture in mediating the long-range connectivity of the HS phase. The HS content of all the PUU copolymers was 22 wt %, and the soft segment (MW 970 g/mol) was a heterofed random copolymer of 50:50 ethylene oxide:propylene oxide, which possesses a single terminal hydroxyl group (monol). An 80:20 isomeric mixture of 2,4- and 2,6-toluene diisocyanate, 4,4′,4″-triphenylmethane triisocyanate and water were utilized during the chain extension step of the synthesis to incorporate HS branching. DSC and SAXS results on the final plaques indicated that the samples were still able to establish a microphase morphology even in the presence of the highest extent of HS branching utilized in the study. The tapping-mode AFM phase image of the PUU sample without HS branching exhibited the presence of long ribbonlike hard domains that percolated through the soft matrix. The long-range connectivity of the HS was increasingly disrupted with higher levels of HS branching. Accompanying such disruption was a systematic mechanical softening of the PUU samples. FT-IR indicated that incorporation of HS branching disrupted the hydrogen-bonded network within the hard phase. These results demonstrate the importance of hydrogen bonding and chain architecture in mediating the long-range connectivity and percolation of the HS and achieving dimensional stability.

1. Introduction

Segmented polyurethane, polyurea, and poly(urethane urea) copolymers are products of the versatile isocyanate chemistry, which was pioneered by Otto Bayer in the late 1930s. A subset of block copolymers, this class of materials is utilized in the production of elastomers, fibers, coatings, overmoldings, components in biomedical and electronic devices, etc.[1,2] Flexible polyurethane foams are also loosely considered to be segmented. The versatility of these materials derives from the wide range of chemical precursors and molecular parameters, such as MW and MWD, which can be selected or manipulated to produce materials with targeted properties. From a structure−property perspective, their ability to develop microphase separation between the soft and the hard segments is one of their most defining features. In segmented copolymers compositionally dominated by the soft segments (SS), the hard segments (HS) can, under appropriate conditions, microphase separate into hard domains. These microphases reinforce the soft matrix by acting as physical cross-link sites. As the relative HS content of the copolymer is raised, the long-range connectivity of the HS is thought to improve and lead to the percolation of the hard phase through the soft matrix. Intersegmental hydrogen-bonding capability of the HS (and the potential crystallizability of the HS if suitable symmetry exists) increases the cohesiveness of the hard domains. However, the role played by hydrogen bonding in enhancing the long-range connectivity of the HS phase is not fully understood.

Scheme 1

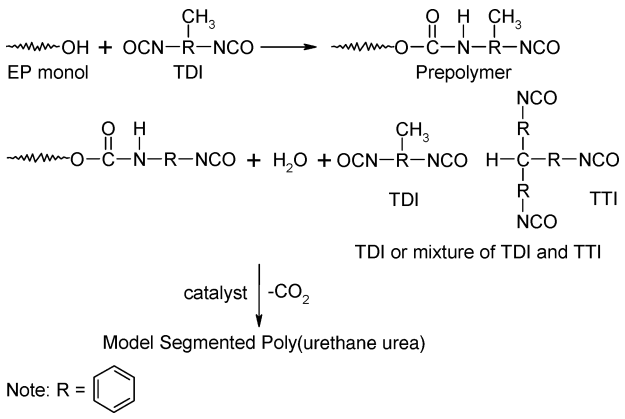

Recent efforts in our laboratory[3] have been directed at understanding the importance of the extent of hydrogen bonding over and above microphase separation in mediating the long-range connectivity of the HS. A model trisegment poly(urethane urea) (PUU) of the type soft−hard−soft was synthesized according to the prepolymer route shown in Scheme 1. A 50:50 ethylene oxide:propylene oxide based monofunctional alcohol,

* To whom correspondence should be addressed. E-mail: gwilkes@vt.edu.

10.1021/ma048222v CCC: $30.25
Published on Web 05/28/2005

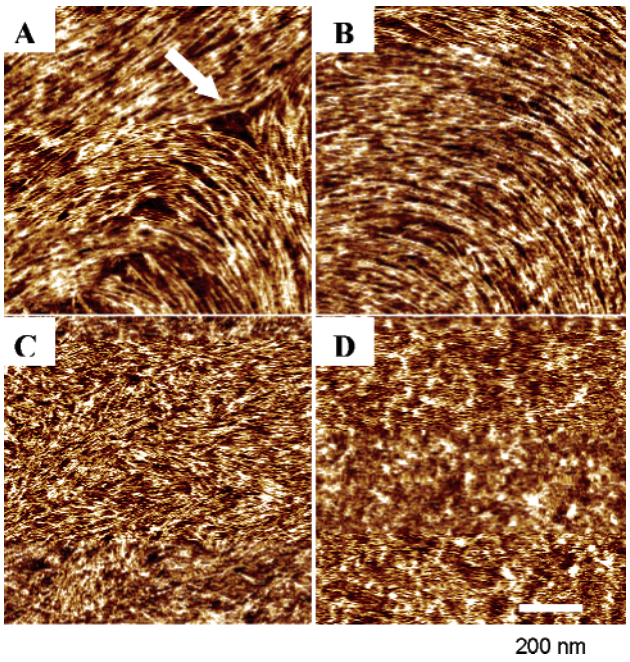

Figure 1. Tapping-mode AFM phase images of solution-cast oligomeric trisegment PUU films with (A) 0.0, (B) 0.1, (C) 1.0, and (D) 1.5 wt % LiCl. Note that all samples contain 22 wt % HS content, and 1.0 wt % LiCl corresponds to an average of 1 LiCl molecule per 4 urea linkages along the HS of the trisegment PUU (reproduced from ref 3). Copyright 2004 Elsevier.

commonly referred to as a monol, of MW 970 g/mol was end-capped with an 80:20 isomeric mixture of 2,4- and 2,6-toluene diisocyanate (TDI). This prepolymer was then chain extended with stoichiometric amounts of TDI and water to yield a 22 wt % HS containing trisegment PUU with an overall MW < 3000 g/mol. Interestingly, this *unentangled* oligomeric trisegment PUU *solidified* and formed a *self-supporting plaque* upon compression molding. The liquid-to-solid transformation was remarkable in light of the relatively low HS content (22 wt %) of the plaque, a lack of a covalent cross-linked network, the oligomeric MW of the trisegments, and the two terminal SS being ca. 100 °C above their "neat" T_g at room temperature. Such behavior strongly suggested the presence of an extensively percolated HS phase reinforcing the soft matrix. Indeed, the tapping mode atomic force microscopy (AFM) phase image of this sample (see Figure 1A, reproduced from ref 3) cast from a 20 wt % solution in dimethylacetamide supported the above hypothesis. In this image ribbonlike hard domains of high aspect ratio that percolate through the soft matrix are clearly observed. The T_g (DSC) of the soft segment phase is −63 °C, which is slightly higher than the neat monol T_g of −75 °C due to the restrictions imposed on the mobility of the SS by the hard domains as well as by isolated HS that may be dissolved in the soft matrix.

We further investigated the importance of the hydrogen-bonded network within the HS phase of this copolymer in mediating the observed long-range connectivity of the HS phase by utilizing LiCl as a molecular probe. From this earlier work (see Figure 1C,D) we learned that increasing the LiCl loading results in a systematic loss of HS phase long-range connectivity, which in turn leads to a systematic softening of the thoroughly dried samples (determined by thermomechanical analysis). We also noted that the addition of LiCl did not, however, influence the extent of microphase separation in the samples; the samples maintained a SS T_g (DSC) between −63 and −61 °C. On the other hand, FT-IR confirmed that LiCl preferentially interacts with the HS phase (see below for further details). Thus, these results indicated that hydrogen bonding plays an important role in promoting structural stability (solidification) in PUU copolymers with a low degree of polymerization.

In this report, we present the results from an investigation in which we probed the role of chain architecture, specifically HS branching, in mediating the long-range connectivity of the HS and the hydrogen-bonded network within the hard phase in the model segmented PUU copolymer addressed above. We incorporated varying extents of HS branching by utilizing different relative ratios of a di- and triisocyanate along with water during the chain extension step of the synthesis, the details of which are given below.

2. Experimental Section

2.1. Materials. A heterofed 50:50 ethylene oxide and propylene oxide based monofunctional alcohol of MW 970 g/mol (EP monol), TDI, 4,4′,4″-triphenylmethane triisocyanate (TTI), and deionized water were used as raw materials along with a conventional catalyst package consisting of 5:1 parts by weight of Dabco 33LV:BL11. Bayer Material Science graciously supplied the EP monol and the isocyanates, TDI and TTI. We used these precursors without further purification. Air Products kindly provided the Dabco catalyst package.

2.2. Synthesis. The synthesis of model segmented PUU copolymers utilized in this study is presented in Scheme 1. To synthesize the prepolymer, 485 g of the EP monol followed by 87 g of TDI was added to a 1 L flame-dried round-bottom flask. After the addition of the reactants, the mixture was stirred vigorously for 30 min and thereafter placed in an oven at 60 °C for 24 h to ensure completion of the reaction; a −NCO peak could not be detected in the FT-IR spectrum of the prepolymer after 5 h. On the issue of the choice of the particular monol, in one of our earlier publications,[4] which utilized monols in linear model copolymers, we obtained similar results when a poly(propylene oxide)-based monol (PP) of MW 1000 g/mol was used instead of EP, also of MW 1000 g/mol. Hence, while indeed the presence of ethylene oxide should affect the soft segment solubility, we have noted no major differences in the final materials when the EP and PP systems were made by the same procedures. Also note that during the prepolymer synthesis the production of the species "monol−TDI−monol" is also possible. However, because of the changes in the resonance stabilization of TDI's phenyl ring and the lower reactivity of the −NCO group at the *ortho* position after the one on the *para* position has reacted (in the case of 2,4-TDI), probability calculations show that the prepolymer should consist of less than ca. 10% "monol−TDI−monol" species. The prepolymer was then allowed to cool to ambient temperature. Small quantities of this prepolymer (ca. 28 g) were then chain extended with deionized water and a mixture of a di (TDI)-functional and tri (TTI)-functional isocyanate. Different ratios of TDI/TTI were utilized to synthesize a total of five segmented PUU with varying extents of HS branching but a fixed HS content of 22 wt %. The HS content of the samples was calculated on the basis of the amounts of TDI, TTI, and water that were utilized during synthesis. The chain extension step was catalyzed with less than 0.2 wt % of the Dabco catalyst package. The reader may recognize that the above synthesis route mimics PUU foam chemistry except that in the present instance we have utilized no surfactants and replaced the trifunctional or higher functional polyol with a monol. We adopted such a route in light of our laboratory's longstanding interest[5−9] in the structure−property behavior of water-blown flexible PUU foams. Generally, in the production of these materials, the reaction of water

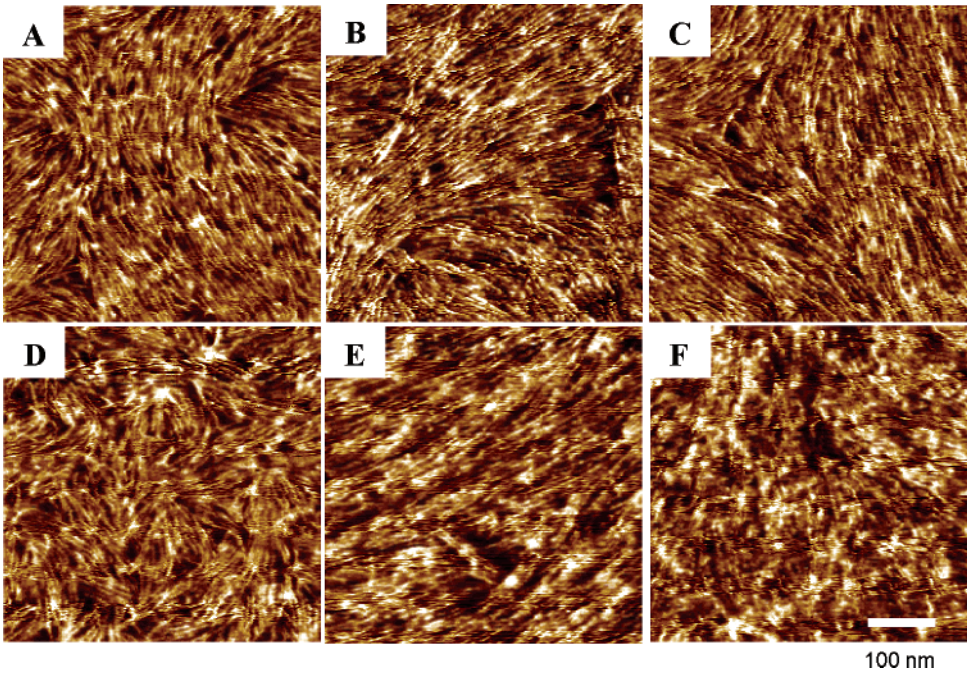

Figure 2. Tapping-mode AFM phase images of segmented PUU solid plaques containing (A) no TTI, this sample is a linear trisegment PUU with overall MW < 3000 g/mol; (B) 0.14; (C) 0.6; (D) 0.8; (E) 1.6; and (F) 2.90 wt % TTI.

with an isocyanate results in the evolution of carbon dioxide, which is utilized as an "in situ" foaming agent. However, in the present study, the reaction mixtures were stirred continuously until the evolution of CO_2 ceased. Each of the resulting segmented PUUs were poured into a picture-frame mold and sandwiched between Teflon sheets and steel plates. This assembly was then placed in a hot press at 100 °C and under 10 000 kg_f for 2 h to ensure completion of the reaction. The resulting solid plaques were stored under vacuum at ambient temperature until used for analysis. The TTI content (and therefore the extent of HS branching) in the copolymers was 0.14, 0.60, 0.80, 1.60, and 2.90 wt %. It may be noted that 0.14 and 2.9 wt % TTI correspond to replacing 1% and 25% of the TDI−NCO groups with TTI−NCO groups, respectively, in the chain extension step of the synthesis. A linear trisegment PUU with 22 wt % HS content, which was synthesized by chain extending the prepolymer with deionized water and TDI alone, was used as a control. Following their polymerization, all six samples were completely soluble in dimethylacetamide, indicating the absence of any gel formation.

2.3. Atomic Force Microscopy. Tapping-mode AFM of the free surface of solid plaques was conducted at room temperature via a Veeco Dimension 3000 scanning probe microscope using Nanosensors' TESP 7 tips with a force constant of 35 N/m. Images were captured at a set-point ratio of ca. 0.6.

2.4. Fourier Transform Infrared Spectroscopy. Using a Nicolet 510 spectrometer FT-IR spectra of thoroughly dried films that were cast from a 20 wt % solution in dimethylacetamide on KBr disks were collected at a resolution of 2 cm^{-1}. A total of 64 scans were coadded to each file, and a background, 64 scans at a 2 cm^{-1} resolution, was collected before each sample run.

2.5. Differential Scanning Calorimetry. DSC of the samples was performed in a Seiko DSC 220C. The samples were quenched from room temperature to −100 °C using liquid nitrogen and thereafter subjected to a heating scan at the rate of 10 °C/min. The experiments were conducted under a dry nitrogen atmosphere.

2.6. Thermomechanical Analysis. Isothermal thermomechanical analysis (TMA) experiments were conducted at room temperature in a Perkin-Elmer DMA 7e by following the penetration of a rounded conical quartz probe into the sample for a period of 10 min. A constant load of 30 mN was applied during each experiment.

2.7. Small-Angle X-ray Scattering. Small-angle X-ray scattering (SAXS) profiles were collected by utilizing a Phillips X-ray generator, model PW1729, operating at 40 kV and 20 mA and generating nickel-filtered Cu Kα radiation with a wavelength of 1.542 Å. The scattering patterns were collected by a Kratky camera with a 0.03 × 5 mm^2 slit collimation in conjunction with a Braun OED50 position-sensitive detector. The raw scattering data were corrected for parasitic scattering and normalized by sample thickness and exposure time. The intensity data were also normalized by using a Lupolen standard.

3. Results and Discussion

Tapping-mode AFM phase images of solid PUU plaques with 22 wt % HS content but varying extents of HS branching are presented in Figure 2. In these phase images, by convention, the hard and soft microphases appear as bright and dark regions, respectively. The linear trisegment PUU (Figure 2A) exhibits long ribbonlike hard domains, which percolate through the soft matrix. Upon comparison of the two phase images in Figures 1A and 2A, we note that both the solution-cast film and the solid plaque respectively possess similar morphologies. Besides the percolated ribbonlike hard domains, a common morphological feature in their respective packing topology is the presence of wall or disclination-like defect (see arrow) in Figure 1A where the ribbons have "turned" to allow for continuation of packing. Such a morphological feature is more commonly observed in nematic liquid crystals.[10] As noted earlier, such an extensively percolated hard phase reinforces the soft matrix and enables the oligomeric sample to solidify into a relatively rigid system. Such morphology also suggests that the HS pack orthogonally to the long axis of the ribbons. A similar packing has also been noted in poly(tetramethylene oxide)-based polyurethanes and polyureas with uniform length HS[10,11] or poly(ether ester aramide)s, also with uniform length HS.[13]

The incorporation of HS branching, up to 1.6 wt % TTI (Figure 2E), does not result in any apparent large-

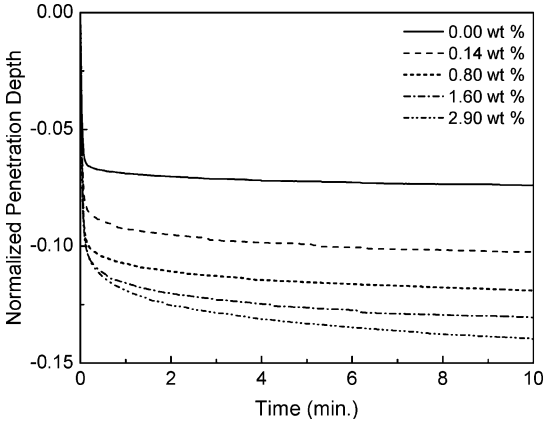

Figure 3. TMA probe penetration in segmented PUU solid plaques containing varying extents of HS branching.

scale disruption of the HS long-range connectivity. However, the limited breakup of the ribbons may result in a broadening in the size distribution of the hard domains. At a TTI loading of 2.9 wt % (Figure 2F) one is still able to note the presence of bright and dark regions that indicate the presence of a microphase morphology. However, the ribbonlike hard domains cannot be clearly discerned, which suggests that incorporation of HS branching makes it increasingly difficult for the HS to pack as efficiently and percolate through the soft matrix. In fact, the extent of HS branching enabled by the incorporation of 4.6 wt % TTI hinders HS packing to such an extent that this sample is unable to solidify, and it remains a viscous liquid. While the disruption of the long-range connectivity of the HS phase upon addition of HS branching is distinct, it is not as striking as was noted in our earlier study[3] for the addition of LiCl to the fully TDI-based system (recall Figure 1).

The direct consequence of the incorporation of HS branching is the systematic softening of the samples as confirmed by TMA. From Figure 3 we observe that the extent of the probe penetration over a period of 10 min increases with increasing TTI content of the sample. The rate of penetration of the probe slows considerably after 2 min because the incorporation of HS branching also raises the overall MW of the sample. This results in an increase in the viscosity of the copolymer, which may partially counterbalance the softening of the sample that would occur due to the loss in HS percolation. On the other hand, in our earlier study the overall MW of the copolymer remained constant because samples with various levels of LiCl were obtained by adding required amount of LiCl to the same starting linear trisegment-based PUU.[3] Thus, in that study, the systematic softening of thoroughly dried samples with increasing LiCl content was more pronounced (data not shown), and the rate of the TMA probe penetration over a period of 10 min was also greater than that noted in the present study.

We further probed the microphase morphology of the copolymers addressed in this study by utilizing SAXS, which is a bulk technique. The slit-smeared SAXS profiles of the six segmented PUU copolymers are presented in Figure 4. As can be observed in Figure 4A, the samples with up to 0.8 wt % TTI content clearly exhibit a shoulder in their respective scattering profiles. These samples exhibit an interdomain spacing or a d spacing, which estimated by Bragg's law is the inverse of the scattering vector s, of ca. 80 Å. The first-order

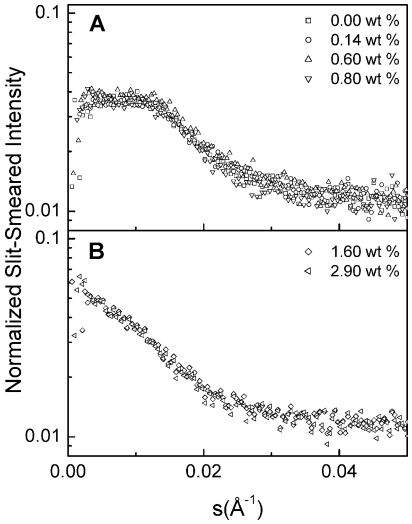

Figure 4. Slit-smeared SAXS profiles of segmented PUU solid plaques: (A) the intensity of profiles of samples with 0.00, 0.15, 0.60, and 0.80 wt % TTI; (B) the intensity of profiles of samples with 1.60 and 2.90 wt % TTI. Copyright 2004 Elsevier.

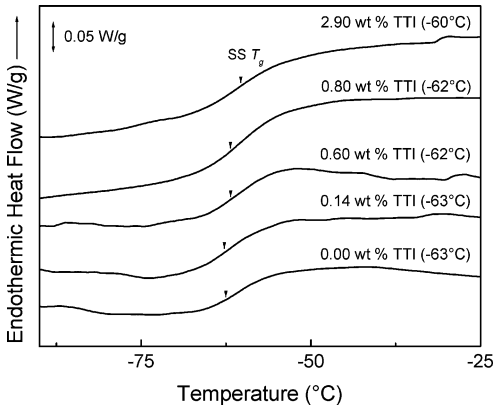

Figure 5. DSC profiles of selected segmented PUU solid plaques. A given sample's T_g is given in rounded brackets next to its TTI content. Note that we did not observe any HS T_g in the six copolymers' DSC heating profiles due to the small heat capacity change exhibited by this phase during its glass transition.

interference shoulder in the scattering profiles of the copolymers with 1.60 and 2.90 wt % TTI (Figure 4B) is distinctly less defined than in the samples with lower TTI content. In light of the similar SS T_g of all six copolymers as observed by DSC (Figure 5), the SAXS response of the two samples with 1.60 and 2.90 wt % TTI suggests that HS branching possibly leads to a broader distribution of the hard domain sizes. In fact, the reader may recall that such behavior was also noted in the respective AFM phase images (Figure 2E,F) of these two samples. Thus, both AFM and SAXS results are consistent with each other.

So far we have demonstrated by utilizing the techniques of AFM and SAXS that the incorporation of HS branching in the model segmented PUU addressed in this study results in the disruption of the HS's long-range connectivity, which in turn leads to a systematic softening of the samples as confirmed by TMA. We also investigated by utilizing FT-IR the impact of HS branching on the state of the hydrogen-bonded network in these model PUU. In the IR region between 1700 and 1600 cm^{-1}, the urea carbonyl (C=O) group can exhibit two absorbance peaks: at 1680 and 1640 cm^{-1} corresponding to loosely hydrogen-bonded and strongly hy-

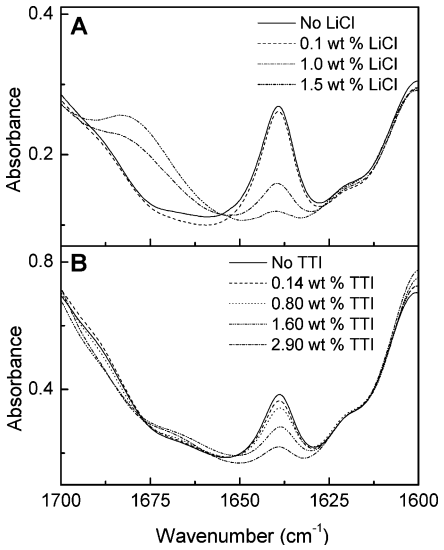

Figure 6. Urea C=O stretching region of the FT-IR spectra of solution-cast films: (A) linear trisegment PUU with LiCl (reproduced from ref 3) and (B) segmented PUU with HS branching.

drogen-bonded C=O, respectively.[14,15] The intensity of these peaks can be used to measure the relative concentration of free and hydrogen-bonded C=O groups. In our earlier study,[3] we noted that the intensity of the bonded peak at 1640 cm^{-1} decreases systematically with increasing LiCl content, and as expected, it is accompanied by a corresponding increase in the intensity of the 1680 cm^{-1} peak (see Figure 6A). Thus, in this earlier work, FT-IR in conjunction with AFM enabled us to demonstrate that such a disruption of the hydrogen-bonded network by addition of LiCl resulted in the loss of the long-range connectivity of the HS phase (see from Figure 1). In the present study, we note from Figure 6B that as the TTI content (or HS branching) of the copolymer increases, the absorbance intensity of the urea bonded peak (1640 cm^{-1}) decreases. Surprisingly, unlike LiCl-doped systems, no increase in the absorbance intensity at 1680 cm^{-1} corresponding to the loosely hydrogen-bonded urea C=O stretching was observed. However, the FT-IR response of these samples in general demonstrates that as the level of HS branching increases, the ability of the HS to pack effectively and establish a hydrogen-bonded network suffers.

4. Conclusions

Model segmented PUU copolymers with varying extents of HS branching were utilized to study the influence of chain architecture on the morphology of these materials. We incorporated HS branching by utilizing a triisocyanate along with a diisocyanate and water during the chain extension step of the synthesis. We controlled the relative ratio of these two isocyanates to synthesize five copolymers with varying extents of branching but a constant HS content of 22 wt %. A linear trisegment also with 22 wt % HS content, which was synthesized by utilizing no triisocyanate during chain extension, was used as a control. This oligomeric sample was able to solidify due to the extensively percolated hard phase, as seen by tapping-mode AFM. However, the incorporation of HS branching reduced the ability of the HS to pack as effectively and establish long-range connectivity. Such disruption resulted in the softening of the copolymers. While the samples are able to retain a microphase morphology in the presence of 2.90 wt % TTI as confirmed by DSC, AFM, and SAXS, the latter two techniques revealed that HS branching possibly induces a broader hard domain size distribution. HS branching also places limitations on the ability of the HS to develop a well-structured hydrogen-bonded network as noted by FT-IR.

Thus, these results demonstrate that both the hydrogen-bonding capability of the HS and the ability of the HS to establish long-range connectivity and percolation through the soft matrix are influenced by the extent of HS branching. In addition, the rigidity or stiffness of the segmented PUU addressed in this study depends on the extent of the HS percolation through the soft matrix.

Acknowledgment. The authors gratefully acknowledge the financial support provided by the U.S. Army Research Laboratory Grant DAAD 19-02-1-0275 under the MAP-MURI program and Emel Yilgor for her assistance during the synthesis of the copolymers utilized in this study.

References and Notes

(1) Legge, N. R., Holden, G., Schroeder, H. E., Eds.; *Thermoplastic Elastomers: A Comprehensive Review*; Hanser Publishers: New York, 1987.
(2) Hepburn, C. *Polyurethane Elastomers*; Elsevier Applied Science: New York, 1992.
(3) Sheth, J. P.; Aneja, A.; Wilkes, G. L. *Polymer* **2004**, *45*, 5979.
(4) Aneja, A.; Wiles, G. L. *Polymer* **2004**, *45*, 927.
(5) Wilkes, G. L.; Abouzahr, S.; Radovich, D. *J. Cell. Plast.* **1983**, *19*, 248.
(6) Armistead, J. P.; Wilkes, G. L.; Turner, R. B. *J. Appl. Polym. Sci.* **1988**, *35*, 601.
(7) Moreland, J. C.; Wilkes, G. L.; Turner, R. B.; Rightor, E. G. *J. Appl. Polym. Sci.* **1994**, *52*, 1459.
(8) Dounis, D. V.; Wilkes, G. L. *Polymer* **1997**, *38*, 2819.
(9) Kaushiva, B. D.; Wilkes, G. L. *Polymer* **2000**, *41*, 6987.
(10) O'Rourke, M. J. E.; Ding, D. K.; Thomas, E. L.; Perec, V. *Macromolecules* **2001**, *34*, 6658.
(11) Aneja, A.; Wilkes, G. L. *Polymer* **2003**, *44*, 7221.
(12) Unpublished results.
(13) Sauer, B. B.; Mclean, R. S.; Gaymans, R. J.; Niesten, M. C. J. E. *J. Polym. Sci., Part B: Polym. Phys.* **2004**, *42*, 1783.
(14) Elwell, M. J.; Ryan, A. J.; Grunbauer, H. J. M.; Lieshout, H. C. *Polymer* **1996**, *37*, 1353.
(15) Sung, C. S. P.; Schneider, N. S. *Macromolecules* **1975**, *8*, 68.

MA048222V